Synchronized measurement technology supported AC and HVDConline disturbance detection

Naglic, M.; Liu, L.; Tyuryukanov, I.; Popov, M.; van der Meijden, M.A.M.M.; Terzija, V.

DOI
10.1016/j.epsr.2018.03.007

Publication date
2018

Document Version
Final published version

Published in
Electric Power Systems Research

Electric Power Systems Research 160 (2018) 308–317

Contents lists available at ScienceDirect

Electric Power Systems Research

journal homepage: www.elsevier.com/locate/epsr

Synchronized measurement technology supported AC and HVDC online disturbance detection

M. Naglic[a,*], L. Liu[a], I. Tyuryukanov[a], M. Popov[a], M.A.M.M. van der Meijden[a,b], V. Terzija[c]

[a] Faculty of Electrical Engineering, Mathematics, and Computer Science, Delft University of Technology, 2628 CD Delft, The Netherlands
[b] TenneT TSO, 6812 AR, Arnhem, The Netherlands
[c] School of Electrical and Electronic Engineering, University of Manchester, Manchester M13 9PL, UK

ARTICLE INFO

Article history:
Received 13 December 2017
Received in revised form 6 March 2018
Accepted 8 March 2018
Available online 26 March 2018

Keywords:
Online disturbance detection
PMU
HVDC
RTDS
Co-simulation

ABSTRACT

In electric power system, disturbance detection has become an important part of grid operation and refers to the detection of a voltage and current excursion caused by the wide variety of electromagnetic phenomena. This paper proposes a computationally efficient and robust algorithm for synchronized measurement technology (SMT) supported online disturbance detection, suitable for AC and HVDC grids. The proposed algorithm is based on the robust median absolute deviation sample dispersion measure to locate dataset outliers. The algorithm is capable of identifying the disturbance occurrence and clearance measurement sample based on the dynamic criteria, driven by present power system conditions. The effectiveness of the proposed algorithm is verified by real-time simulations using a cyber-physical simulation platform, as a co-simulation between the SMT supported electric power system model and underlying ICT infrastructure. The presented results demonstrate effectiveness of the proposed algorithm, making it suitable for an AC and HVDC online disturbance detection application or as a pre-step of backup protection schemes.

1. Introduction

In the recent years, the Smart Grid technological advances in terms of sophisticated intelligent electronic devices (IED), fast and reliable telecommunication links, and increased computational capacities have created new opportunities for design of advanced protection schemes [1].

Typically supported by a global navigation satellite system, the synchronized measurement technology (SMT) makes use of IEDs with specialized firmware or phasor measurement units (PMU) to deliver time-synchronized system-wide measurements in real-time [2,3]. SMT is the key element of wide area monitoring protection and control (WAMPAC) system [4,5], which is favourable to ensure a higher system stability and reliability.

1.1. Paper motivation

Nowadays, the power systems undergoes major changes towards a heterogeneous, widely dispersed, yet globally interconnected system with large-scale integration of distributed energy resources [6,7]. Due to the decreased system inertia and higher uncertainty associated with renewable energy sources, the power system have become more vulnerable, especially in terms of power quality and security of supply [8]. Without in-time remedial action, a severe disturbance can lead to a malfunction or break-down of hardware components and considerable economical loss, or, in the worst case scenario, to a complete power system blackout.

Therefore, adequate disturbance detection has become an important part of power system operation and protection and refers to the detection of a voltage and current excursion caused by a wide variety of electromagnetic phenomena [9]. An important requirement for disturbance detection techniques is to provide online, fast, and reliable detection of disturbances that potentially endanger the safe operation of electric power system.

A significant amount of work has been done to locally detect and monitor the grid operating conditions by leveraging the information extracted from signal samples [10,11]. The available disturbance detection methods can be generally classified into two groups. The first group consists of digital signal processing techniques, where the wavelet transform (WT) [12–15], Fourier transform [16,17] and S-transform [18,19] based methods are dominating. However, these methods require either a high

* Corresponding author.
E-mail address: m.naglic@tudelft.nl (M. Naglic).

https://doi.org/10.1016/j.epsr.2018.03.007

measurement sampling rate or a long observation time interval associated with complex mathematical operations, thus making them less appropriate for real-time operation. In fact, WT based techniques are proven to perform well in identifying singularities in the decomposed signal components [20–22]; although the precise time localization of a transient can be ensured, the WT techniques are in general computationally costly, noise sensitive, and their performance depends on the utilized mother wavelet. On the other hand, the statistical techniques [23–25] are often less complex and computationally more efficient. However, many presented methods are prone to false-trigger events due to the fixed threshold used to identify a disturbance. The remaining challenge is to dynamically tune the disturbance identification threshold based on the present system conditions.

With the development of PMU, there was a parallel development of backup protection schemes utilizing the advantages of SMT. Authors in Ref. [26] make use of the characteristic ellipsoid method and a decision tree technique to monitor dynamic system behaviour, identify system events and their location. Although the results are promising, the heavy computational burden makes the algorithm not suitable for real-time operation. In Ref. [27] authors perform principal component analysis to predict the measurement trend and detect abnormalities resulting from unexpected sudden changes. Similarly, a centralised disturbance detection scheme was recently presented, based on the grid parameter estimation technique [28]. The impact of data drop and ICT delay on disturbance detection was also discussed. However, both papers fail to detail the disturbance identification threshold value.

1.2. Paper contributions

This paper proposes a novel SMT-supported online disturbance detection algorithm, which can be utilized as a pre-step of AC and HVDC protection schemes or an online disturbance monitoring application. The proposed disturbance detection algorithm is based on the median absolute deviation (MAD) sample dispersion method, which is a robust statistical measure of univariate dataset variability. The emphasis of the proposed algorithm is on fast response and low computational burden, making it suitable for the online operation. The algorithm is shown to be capable of detecting disturbances in AC and HVDC grids, which are seen as sudden deviations (short-duration dips, swells, interruptions) in the SMT measurements. Disturbances include but are not limited to short circuit faults, line trips and reclosing actions, and large loss of generation or load. Each identified disturbance is characterized with the start and end measurement sample of disturbance occurrence and clearance respectively. To the best authors' knowledge, this paper for the first time makes use of PMUs to deliver time synchronized measurements of HVDC grid.

The effectiveness of the proposed algorithm is verified by real-time simulations using a cyber-physical simulation platform and a small test system model, which includes an HVDC multi terminal configuration based on the modular multilevel converter (MMC) technology. The simulations are performed on the RTDS® real-time power system simulator with integration of the actual SMT components and online disturbance detection center (DDC) as software-in-the-loop.

The aim of this paper is to present a novel SMT-supported online disturbance detection algorithm and its performance capabilities for AC and HVDC. The remainder of the paper is organized as follows: Section 2 presents the data acquisition for AC and HVDC systems. Section 3 presents the algorithm formulation applied to process the data and detect disturbance. Section 4 demonstrates the cyber-physical simulation platform and the used power system model. Section 5 presents the results and discussion. Finally, Section 6 concludes the paper.

2. Data acquisition

In a power system, a voltage or current oscillation signal can be expressed as a sum of complex sinusoidal signals and noise, as:

$$x(t) = \sum_{k=1}^{n} A_k e^{-\sigma_k t} \cos(\omega_k t + \phi_k) + \varepsilon_k(t) \tag{1}$$

where $n \in \mathbb{N}$ is total number of signal components, A is amplitude, σ is damping ratio, ω is angular frequency, ϕ is phase, and ε represent noise and DC decaying offset of each signal component.

Typically, bus waveform signals are fed through adequate current and voltage transformers to the waveform input channels of a PMU device [4]. Recently, several papers [29,30] were published about the digital signal processing methods for a PMU synchrophasor estimation. Through these methods, voltage and current synchrophasors of the fundamental frequency component and the instantaneous system frequency can be determined from waveform samples.

In order to extend the proposed approach to disturbance detection on an HVDC grid, the IEEE Standard C37.118 messages are exploited as a medium for transferring time-synchronized HVDC measurements. In this case, the HVDC voltage and current analog signals of appropriate levels are fed into PMU multi-functional analog input channels. The signal (voltage and current) magnitudes are sampled and transferred as "single point-on-wave" values in 16-bit integer or IEEE floating-point format [2]. Since the analog signal sampling (in case of a GTNET PMU) is done after the synchrophasor estimation (windowing), it is prudent to delay the HVDC input signals for the duration equal to the half of the synchrophasor estimation window length (group delay compensation [2]) as:

$$\tau_{analog} = \frac{N}{2Fsf_0} \tag{2}$$

where N denotes the windowing filter order, Fs is the ADC sampling rate (samples/cycle), and f_0 is the nominal system frequency. In this way, the HVDC measurement sampling is time-aligned with the AC synchrophasor estimation timestamp.

In general, any measured signal of interest can be exploited for disturbance detection. In this paper, the instantaneous positive sequence voltage magnitude and the HVDC voltage magnitude measurements are used for AC and HVDC respectively. In this way, only one source of measurements (positive sequence) can be used to detect single-phase and multi-phase AC disturbances.

3. Methodology

It is assumed that in an electric power system only the N_b buses of interest are monitored with a PMU device. With M being the total number of most recent past measurements (samples) within the observation time interval (window), the samples (measurements of interest) to be examined are defined as $x_{i,k}$ where $k = 1, 2 \ldots M$, $\in \mathbb{R}^M$ and $i = 1, 2, \ldots N_b$, $\in \mathbb{R}^{N_b}$ also called the sample vector $X_i = \left[x_{i,1}\, x_{i,2} \ldots x_{i,M}\right]$ of bus i. The dataset containing sample vectors from all N_b buses is presented by the following time series matrix W, as:

$$W = \begin{bmatrix} X_1 \\ X_2 \\ \vdots \\ X_{N_b} \end{bmatrix} = \begin{bmatrix} x_{1,1} & x_{1,2} & \cdots & x_{1,M} \\ x_{2,1} & x_{2,2} & \cdots & x_{2,M} \\ \vdots & \vdots & \ddots & \vdots \\ x_{N_b,1} & x_{N_b,2} & \cdots & x_{N_b,M} \end{bmatrix} \in \mathbb{R}^{N_b \times M} \tag{3}$$

In this paper, MAD is used as a robust sample dispersion measure to locate the X_i sample vector outlier samples [31]. MAD is similar to the well-known standard deviation, but it is more appropriate for screening outliers, due to its robustness to outliers. $MAD_{i,k}$ is defined as a median of the absolute deviations from each $x_{i,k}$ sample and the median of the whole X_i sample vector, as:

$$MAD_{i,k} = median\left(|x_{i,k} - median\left(X_i\right)|\right) \tag{4}$$

The combination of sample median and MAD builds a sturdy method for screening of X_i sample vector outliers, as:

$$X\_mad_{i,k} = \left(x_{i,k} - median\left(X_i\right)\right)/MAD_{i,k} \tag{5}$$

where $X\_mad_{i,k}$ represents the MAD-denominated matrix of samples, defined as deviations of each $x_{i,k}$ sample from the median of the whole X_i sample vector, and divided by the corresponding $MAD_{i,k}$ sample value. In this way, the $X\_mad_{i,k}$ sample value serves to identify the corresponding $x_{i,k}$ outlier, and $X\_mad_{i,k}$ sample polarity (±) to identify the $x_{i,k}$ outlier direction.

The proposed online disturbance detection algorithm consists of two operational modes. The first mode is used to identify a disturbance occurrence moment. The disturbance-affected $x_{i,k}$ sample (outlier) is flagged when the corresponding $X\_mad_{i,k}$ surpass the dynamically determined threshold. This mode operates online and reports a detected disturbance "immediately" after its occurrence. As soon as the disturbance is identified, the algorithm switches into the second operation mode to identify a disturbance clearance. Similarly, the disturbance clearance is identified after the $X\_mad_{i,k}$ samples stabilise below the dynamically determined threshold. It may happen that the disturbance is permanent (line switching actions, generator or load loss), therefore the second operation mode is time-limited and automatically switches into the first mode after a predefined timeout. In this case, the disturbance clearance is reported for a moment after a system reaches a new stable point. Although the algorithm is executed in online fashion, the disturbance clearance moment is reported with a delay due to the algorithm's waiting timeout for a possible disturbance clearance moment.

3.1. Disturbance occurrence identification

In the first mode, algorithm is screening for $x_{i,k}$ samples, seen as outliers compared to the rest of X_i vector samples. For the disturbance occurrence identification it is prudent to take into account only the $X\_mad_{i,M}$ most recent sample value of each observation window and save it into a dynamically erected $mad\_r_{i,t}$ matrix, where index t is used to identify the most recent window calculation, as:

$$mad\_r_{i,t} \quad = X\_mad_{i,M} = \left(x_{i,M} - median\left(X_i\right)\right)/MAD_{i,M} \tag{6}$$

In this way, $mad\_r_{i,:}$ matrix is determined, which consists of the most recent sample $X\_mad_{i,M}$ from each observation window for each monitored bus i. In similar way, the first (least recent) $X\_mad_{i,1}$ window sample is saved into a dynamically erected $mad\_l_{i,t}$ vector for the further use as:

$$mad\_l_{i,t} = X\_mad_{i,1} = \left(x_{i,1} - median\left(X_i\right)\right)/MAD_{i,1} \tag{7}$$

In order to identify a disturbance and determine whether the most recent window sample $x_{i,M}$ is affected by the disturbance, a dynamically defined threshold is applied. The $tr\_start_{i,t}$ threshold is twofold and consists of a dynamically determinated cut-off value based on the medium of the least 25 samples (half window) of $mad\_l_{i,:}$ absolute estimations and multiplied by a user-determinated *factor* parameter to control the algorithm's measurement noise resistance (8). The $tr\_start_{i,t}$ threshold is dynamically determinated based on the previous window $mad\_l_{i,t}$ samples, for each monitored bus i separately. Moreover, the $tr\_start_{i,t}$ threshold is lower-bounded with the user-determined *limit* parameter to control the algorithm's disturbance identification sensitivity, as:

$$tr\_start_{i,t} = \max(mean|mad\_l_{i,t-M\ldots}mad\_l_{i,t-(M/2)}|*factor,\ limit) \tag{8}$$

Based on the performed simulations, the *factor* value of 15 and *limit* value of 15 work generally well for supressing the undesired disturbance identification in case of measurement noise and small load fluctuations respectively. Of course these parameters should be user-adjusted in case of severe sample variance (measurement noise) under normal operation conditions, or load fluctuations.

If the following condition is satisfied, the $D\_start_{i,t}$ disturbance detection start trigger is set:

$$D\_start_{i,t} = \begin{cases} 1, & |mad\_r_{i,t-1} - mad\_r_{i,t}| \geq tr\_start_{i,t} \quad \wedge \\ & |mad\_r_{i,t}| \geq tr\_start_{i,t} \\ 0, & else \end{cases} \tag{9}$$

As can be seen from (9) the most recent $mad\_r_{i,t}$ sample values are compared to $tr\_start_{i,t}$, determined using past $mad\_l_{i,:}$ sample values. As soon as the disturbance on bus i is identified (9) and reported, the proposed algorithm for the corresponding bus i switches into the second operation mode to start with the disturbance clearance identification procedure.

3.2. Disturbance clearance identification

Disturbance clearance identification can be seen as a mirrored procedure of the disturbance occurrence identification. In a similar way, a disturbance clearance moment (11) is identified as soon as the $mad\_l_{i,:}$ vector samples fall below $tr\_end_{i,t}$ dynamically determined threshold (10), as:

$$tr\_end_{i,t} = \max(mean|mad\_r_{i,t-(M/2)}\ldots mad\_r_{i,t}| * factor,\ limit) \tag{10}$$

where *limit* and *factor* parameters are the same as in the case of Eq. (8). If the following condition is satisfied $D\_end_{i,t}$ disturbance detection end trigger is set:

$$D\_end_{i,t} = \begin{cases} 1, & |mad\_l_{i,t-1} - mad\_l_{i,t}| \geq tr\_end_{i,t} \quad \wedge \\ & |mad\_l_{i,t}| \geq tr\_end_{i,t} \\ 0, & else \end{cases} \tag{11}$$

From the moment of disturbance occurrence identification, the proposed algorithm is searching for the disturbance clearance moment for a time period of 5 window lengths. Afterwards, the algorithm switches back into the first mode to continue with disturbance detection identification procedure.

3.3. Operation procedure

In this paper, the dataset W (3) to be examined is limited to 1 s of samples, which corresponds to $M = 50$ most recent PMU measurements of each monitored bus i. In general, the following rule applies: sensitivity of the proposed algorithm to slow magnitude changes increases with the increasing window length, while on the other hand shorter window length makes the algorithm more adaptive to system conditions and suitable for detection of rapid changes. Assuming the application of protection, where a disturbance should be detected as quickly as possible in order to perform a required immediate action, the proposed disturbance detection algorithm operates in online fashion, being executed every time (~20 ms) the W is updated with the set of new PMU measurements.

The following Algorithm 1 pseudocode illustrates the proposed disturbance detection implementation procedure.

Algorithm 1. Online disturbance detection

```
## initialization
t = 1; //index of current window W
D_start_hold_i = false; //dist. present/clear flag
## online processing
while 1
  update W //update dataset (3)
  for i = 1...N_b //processing for bus i
    mad_r_{i,t} //(6)
    mad_l_{i,t} //(7)
    if t > M //collect enough data for (8),(10)
      ## dist. start scan - Mode 1
      tr_start_{i,t} //(8)
      if D_start_{i,t} == 1 and D_start_hold_i == false //(9)
        ## ALERT, dist. detected
        D_start_hold_i = true; //dist. present flag
        D_start_window_i = t; //dist. window index
        D_start_sample_i = x_{i,k}; //dist. start sample
      elseif D_start_hold_i == true //dist. detected?
        ## dist. end scan - Mode 2
        tr_end_{i,t} //(10)
        if D_end_{i,t} == 1 and t < D_start_window_i + 5 * M
        //looking for 5 window lengths (11)
          D_end_sample_i = x_{i,k} //dist. end sample
        else //disturbance end scan finished
          D_start_hold_i = false //dist. clear flag
        endif
      endif
    endif
  endfor
  t = t + 1; //increase current window index
endwhile
```

4. Simulation platform

In order to demonstrate performance capabilities of the proposed algorithm, the cyber-physical simulation platform [32] is utilized, as a co-simulation between the SMT supported electric power system model and underlying ICT infrastructure in real-time.

4.1. Power system model

The disturbance detection algorithm is evaluated on the power system model (Fig. 1), composed of a 4 terminal MMC-based HVDC and 50 Hz nominal frequency AC grid. The model configuration is displayed in Fig. 1. All the 201-level MMC converters are Type-4 model [33] with the setpoints listed in Table 1.

In addition, a circulating current suppression controller is implemented to deal with a voltage imbalance in sub-modules on each arm. The voltage level of the HVDC network is controlled to operate at ±200 kV, while the winding ratios of interface transformers Tr-1/Tr-2 and Tr-3/Tr-4 are 220/380 kV and 220/145 kV respectively.

4.2. Cyber-physical simulation platform

The presented power system model (Fig. 1) was first implemented in RSCAD and then simulated in real-time using the RTDS® power system digital simulator (Fig. 2). Furthermore, GTNETx2 based 4 PMUs of class P with 50 fps reporting rate are installed on the both MMC sides to deliver AC and HVDC measurements. Additionally, for the algorithm evaluation purpose, two PMU analog input channels are used to deliver actual timestamps of fault occurrence and clearance. Moreover, to provide accurate time synchronization the GE RT-430 grand master clock is used to deliver the Inter-Range Instrumentation Group code B (IRIG-B) protocol based timestamp signal to the GTSYNC card. Additionally, the master clock provides IEEE 1588 Precision Time Protocol (PTP) time synchronization to the SEL-5073 Phasor Data Concentrator (PDC) and PC running DDC. Further, the PMU-generated measurements are sent over the WANem telecommunication network emulator (possible to emulate packet delay, jitter, and loss) to the SEL-5073 PDC, where the measurements are time-aligned and aggregated into a single IEEE Std. C37.118 data stream. The latter is send over a Local Area Network (LAN) to the MATLAB-based Synchro-measurement Application Development Framework (SADF) [34] (as presented in Fig. 2), where the disturbance detection algorithm is implemented as DDC and executed in an online fashion. It is important to note that all the platform components are precisely time synchronized to evaluate the time difference between a fault occurrence and DDC disturbance detection.

4.3. Online Synchro-measurement Application Development Framework

The proposed disturbance detection algorithm is implemented using the in-house developed SADF library [34], which is used to design and validate SMT supported applications in real-time. The SADF connects to a PDC data stream and parses the IEEE Standard C37.118.2 measurements [2] in an online fashion into a user-friendly format, making it available for user-defined MATLAB applications (Fig. 3).

5. Results and discussion

The proposed algorithm is verified on the presented benchmark model under different conditions. The time difference between the fault occurrence and DDC disturbance detection equals to the sum of the data acquisition and processing latency, and the moment of fault occurrence with respect to the PMU windowing and measurement reporting (further discussed in Sub-section 5.2.1).

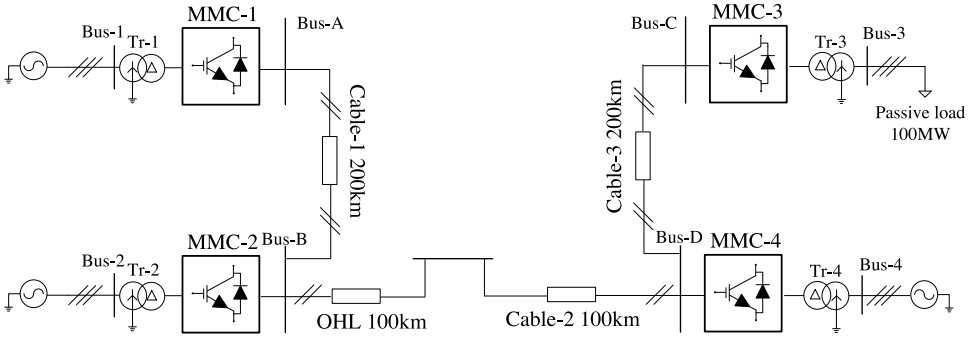

Fig. 1. Four-terminal test AC and HVDC system model.

Table 1
System control mode and set points.

AC system		HVDC system	
Bus name	RMS voltage	Converter name	Control mode and setting points
Bus-1	380 kV	MMC-1	P/V_{dc}; P_{ref} = 400 MW, V_{dc_ref} = ±200 kV, droop = 0.2 Q; Q_{ref} = 0 MVAR
Bus-2		MMC-2	P/V_{dc}; P_{ref} = −800 MW, V_{dc_ref} = ±200 kV, droop = 0.2 Q; Q_{ref} = 0 MVAR
Bus-3	145 kV	MMC-3	Island mode; V_{ac_ref} = 145 kV, frequency = 50 Hz
Bus-4		MMC-4	P; P_{ref} = 500 MW Q; Q_{ref} = 0 MVAR

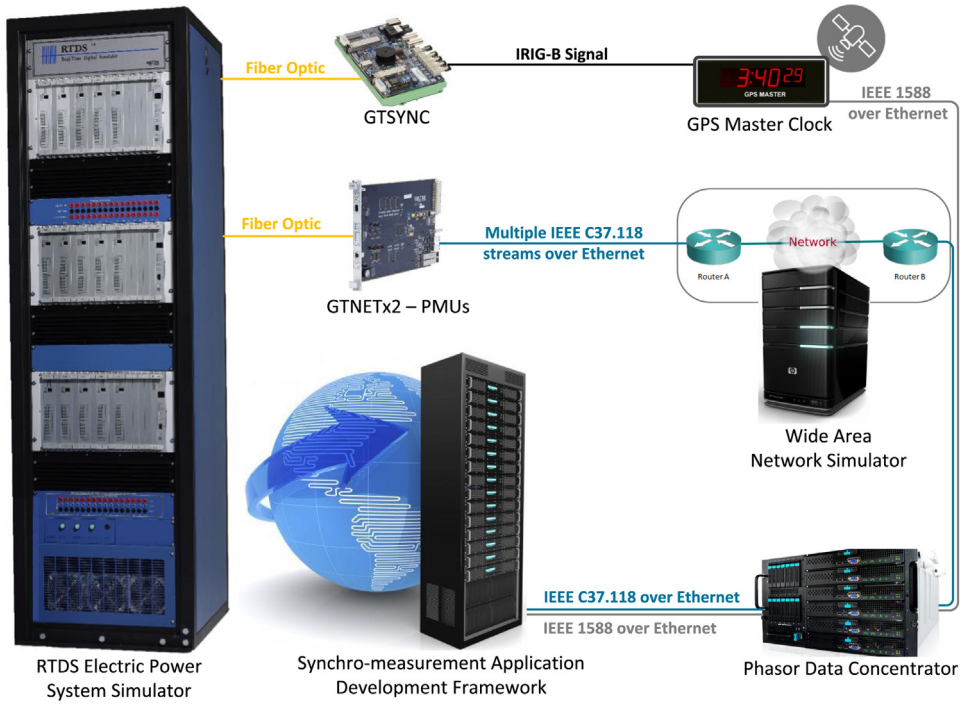

Fig. 2. Real-time based test platform with online disturbance detection algorithm implemented as software-in-the-loop.

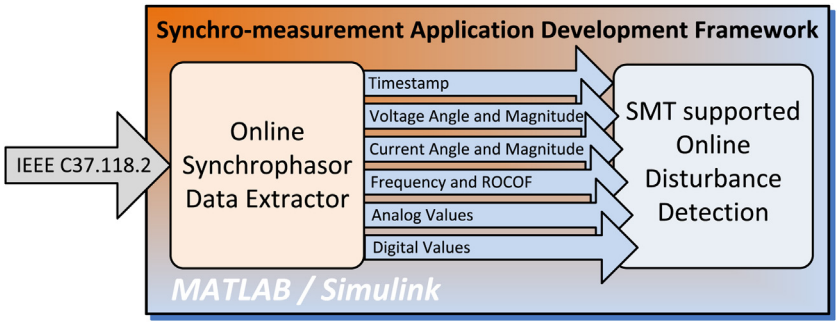

Fig. 3. MATLAB supported Synchro-measurement Application Development Framework, used to implement the proposed disturbance detection algorithm.

5.1. Platform latency evaluation

The τ_{total} platform latency corresponds to the sum of delays imposed by data acquisition and processing:

$$\tau_{\text{total}} = \tau_{\text{PMU}} + \tau_{\text{PMU-PDC}} + \tau_{\text{PDC}} + \tau_{\text{PDC-SADF}} + \tau_{Java} + \tau_{\text{SADF}} + \tau_{\text{DDC}} \quad (12)$$

where τ_{PMU} is PMU windowing and processing delay, $\tau_{PMU-PDC}$ is ICT delay between PMU, WANem and PDC, τ_{PDC} is PDC processing delay, $\tau_{PDC-DDC}$ is ICT delay between PDC and SADF, τ_{Java} is response time of Java I/O-TCP/IP socket implementation (MATLAB Instrument Control Toolbox version 3.11), τ_{SADF} is SADF parsing time of IEEE Standard C37.118.2-2011 messages, τ_{DDC} is processing time related to the disturbance detection algorithm. The approximate platform time delays are listed in Table 2.

5.2. Self-cleared short circuit faults

Performance capabilities of the proposed algorithm are evaluated on voltage sag disturbances caused by self-cleared phase-

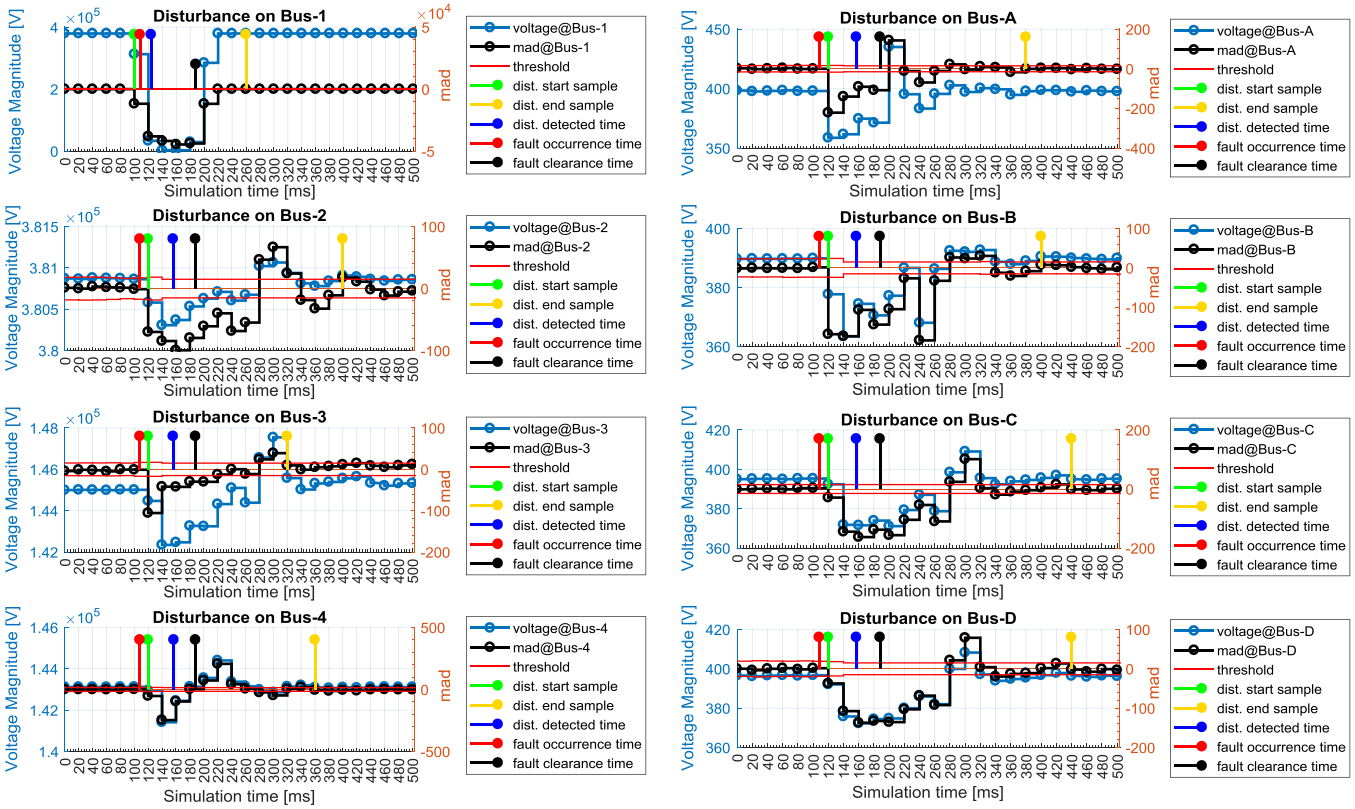

Fig. 4. A three-phase line-to-ground fault on Bus-1 and self-cleared after 80 ms, observed as disturbance on all the busses. (For interpretation of the references to colour in the text, the reader is referred to the web version of this article.)

Table 2
Platform delays.

Delay source	Time range
τ_{PMU}	~21 ms
$\tau_{PMU-PDC}$	~0.4 ms
τ_{PDC}	~0.6 ms
$\tau_{PDC-DDC}$	~0.4 ms
τ_{Java}	between 0 ms and 18 ms
τ_{parse}	~0.7 ms per PMU
τ_{DDC}	~0.02 ms per X_i

to-ground short circuit faults on Bus-1 and Bus-3 and pole-to-pole and pole-to-ground short circuit faults on Bus-B and Bus-D respectively and summarized in Table 3.

Each simulation case contains additional three scenarios with varying short circuit resistance and self-clearing fault times. As presented in Table 3, the disturbance was successfully detected on the faulted bus in all the cases. In order to keep the paper concise, only a limited number of simulation results is graphically presented.

5.2.1. Case A, scenario 1

Fig. 4 presents the disturbance, initiated by a 3-phase line-to-ground fault with 0.001 Ω resistance on Bus-1, and self-cleared after 80 ms. The fault occurrence and clearance time are indicated with the red and black stem respectively. The blue line represents the voltage magnitude, while the black line represents the combined $mad\_r_{i,t}$ and $mad\_l_{i,t}$, before and after disturbance respectively. Similarly, the red line represents the combined $tr\_start_{i,t}$ and $tr\_end_{i,t}$ threshold, before and after disturbance respectively. The measurement sample at which the proposed algorithm identified the disturbance is marked with the green stem, while the disturbance end measurement sample is marked with the orange stem. The moment in time (simulation time) when disturbance was detected is marked with the blue stem respectively. For the sake of simplified interpretation, the actual PMU measurement timestamp ('HH:MM:SS.FFF dd.mm.yyyy' format) has been modified into simulation time, starting with 0 ms for 6th measurement sample before the disturbance identification (green stem).

As seen from Fig. 4, the disturbance was first detected on Bus-1. Due to the nature of PMU sampling, windowing, and measure-

Table 3
Study cases.

Grid	Case	Scenario								
		1: Rf = 0.001 Ω			2: Rf = 10 Ω			3: Rf = 100 Ω		
		Fault duration [ms]								
		1	80	200	1	80	200	1	80	200
AC	A: 3P-G@Bus-1	√	√	√	√	√	√	√	√	√
	B: 1P-G@Bus-3	√	√	√	√	√	√	√	√	√
HVDC	D: P-G@Bus-B	√	√	√	√	√	√	√	√	√
	E: P-P@Bus-D	√	√	√	√	√	√	√	√	√

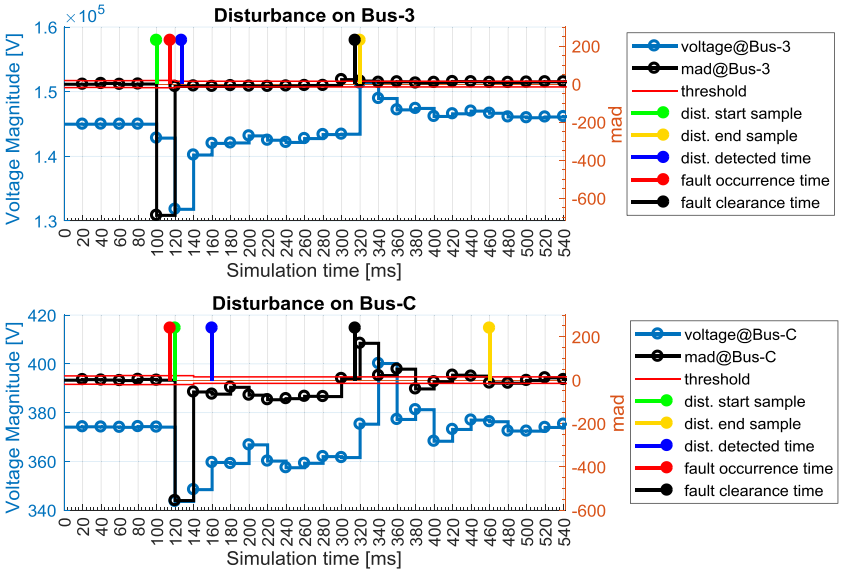

Fig. 5. A single-phase line-to-ground fault, initiated on Bus-3 and self-cleared after 200 ms. (For interpretation of the references to colour in the text, the reader is referred to the web version of this article.)

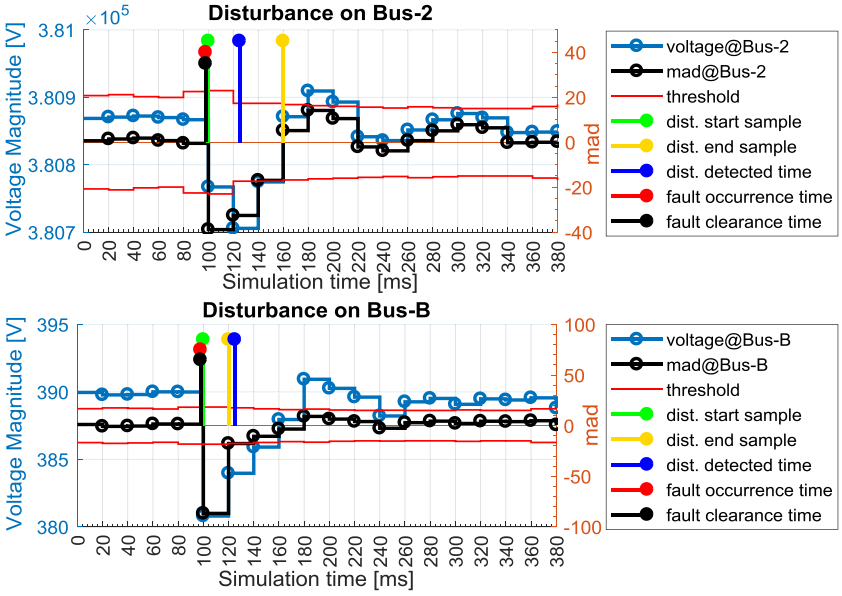

Fig. 6. A pole-to-ground fault on Bus-B and self-cleared after 1 ms. (For interpretation of the references to colour in the text, the reader is referred to the web version of this article.)

ment timestamping, the disturbance-affected PMU measurement sample (green stem) seems to report the disturbance, caused by the fault before the fault actually occurred (red stem). This has practical causes since the PMUs estimate synchrophasors with a 2-cycle window length, with a measurement timestamp corresponding to the time of an observation window centre. Therefore, if the fault-affected waveform samples are present in the second half of the PMU synchrophasor estimation window, they also affect the corresponding resulting synchrophasor measurement with the measurement timestamp before the fault actually occurred.

The disturbance imposed by the single-phase line-to-ground fault on Bus-1 was successfully detected on all buses. The disturbance on Bus-1 was detected with a 21.75 ms delay, caused by data acquisition and processing. On the other buses the disturbance start moment was detected with 53.76 ms delay due to disturbance propagation and the way it affected the PMU sampling (windowing) with respect to measurement reporting. In this simulation case, a 3 ms and 12 ms delay were introduced by τ_{Java} on Bus-1 and the remaining buses respectively. The disturbance end moment (orange stem) for each bus was identified as soon as the $mad\_l_{i,:}$ vector samples fall below $tr\_end_{i,t}$ dynamically determined threshold (10).

5.2.2. Case B, scenario 3

Fig. 5 presents the single-phase line-to-ground fault with 100 Ω resistance, initiated on Bus-3 and self-cleared after 200 ms. The disturbance was identified (blue stem) on Bus-3 with 12.26 ms delay after the fault occurrence (red stem). On Bus-C the disturbance was identified during the next measurement interval.

5.2.3. Case D, scenario 1

Fig. 6 presents a pole-to-ground fault with 0.001 ohm resistance initiated on Bus-B and self-cleared after 1 ms. The disturbance caused by the fault was detected (blue stem) 27.21 ms after the fault

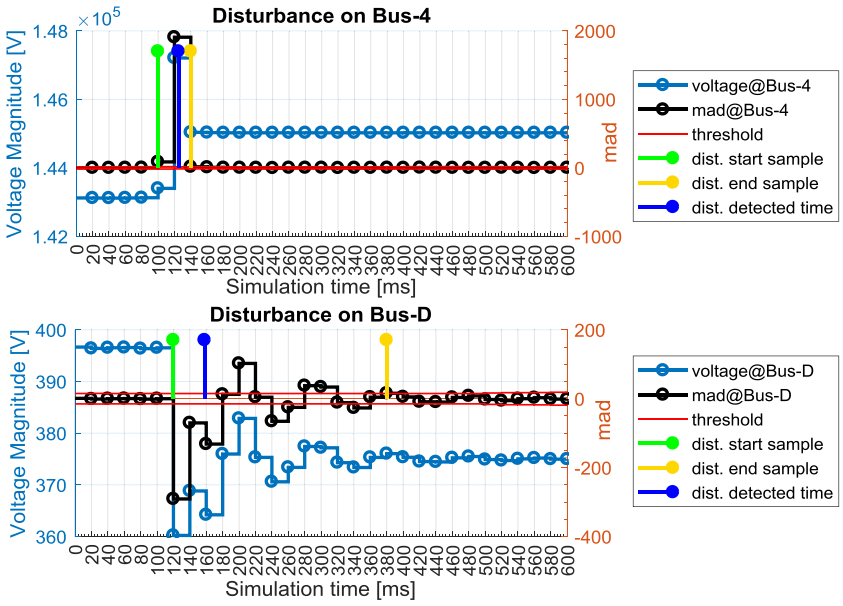

Fig. 7. A disturbance caused by the permanent generation trip.

occurrence (red stem) by the PMUs on Bus-2 and Bus-B. As illustrated on Fig. 6, the dynamic threshold (8) to detect the disturbance start sample (9) has automatically adjusted to the past system conditions (7). Similarly, the dynamic threshold (10) to detect disturbance end sample (11) has automatically adjusted to the most recent system conditions (6), characterised by the measurement data variance.

5.3. Generation loss

The next simulation case shows the detection of disturbance caused by the permanent disconnection of the 500 MW generator machine installed at Bus-4. The disturbance, caused by opening of the circuit breaker, installed between Bus-4 and Tr-4, is presented in following Fig. 7. The disturbance end sample was identified when the measurement samples stabilised below the dynamically defined threshold.

5.4. Comparison with the existing techniques

The performance of the proposed algorithm was compared with the most commonly used WT techniques for disturbance identification. For this, discrete wavelet transform (DWT) and stationary wavelet transform (SWT) methods with the Haar mother wavelet were implemented and executed online using SADF. Hereby, only the execution time to determine (6)–(7) of the proposed method and first level signal decomposition of SWT and DWT is compared. Fig. 8 presents the disturbance, initiated by a self-cleared (80 ms) 3-phase to ground fault on Bus-1. The figure presents the response of the above methods on the disturbance. In the case of DWT, the detail coefficients are down-sampled by the factor of 2 compared to the original signal. This has practical merits due to time-invariant properties of DWT, which should be taken into account. However, this effect is not present in case of SWT due to the zero-padding of high-pass filters coefficients.

Moreover, the median execution time of each method to process one sample window (50 samples) is presented in Table 4.

Based on the presented results in Table 4, the proposed method outperforms SWT and DWT in execution speed for the factor of 25 and 17.5 respectively. Additionally, as seen from Fig. 8 the proposed method captured the disturbance behaviour better compared to the other two methods. In case of SWT, a small transition can be observed at t = 5 s, which has no direct connection to the raw measurements and can be seen as a side effect (anomaly) of SWT processing of the abrupt transition that follows.

Table 4
Execution time.

Method	Median execution time
Proposed method	0.02 ms
SWT	0.50 ms
DWT	0.35 ms

5.5. Discussion

The above presented results demonstrate effectiveness of the proposed algorithm for the disturbance detection caused by different faults, generation disconnection, and line trip. Based on the simulations performed on a typical office personal computer, the disturbance detection algorithm outperforms the WT based techniques in terms of execution time. This is an important property in case of a large number of monitored buses. Similarly to WT-based techniques, the proposed method can be used for a disturbance polarity detection, which is often used as a pre-step of protection schemes. As demonstrated, PMUs can be successfully utilized for delivery of time-synchronized HVDC grid measurements. It is important to note that latency between the disturbance occurrence and its detection variates with respect to the fault occurrence moment (relative to the centre of PMU observation window), PMU synchrophasor estimation algorithm (its window length and complexity), measurement reporting rate, ICT data transmission latencies, and delays introduced by PDC and DDC data processing. Particularly, the τ_{Java} delay, introduced by MATLAB (Java), could be minimised/omitted if the parsing of IEEE Standard C37.118 measurements and proposed algorithm are implemented in Sub-section 5.3, or similar high-performance programming language.

6. Conclusions and future work

This paper presented a novel computationally efficient and robust algorithm for the SMT-supported online disturbance detec-

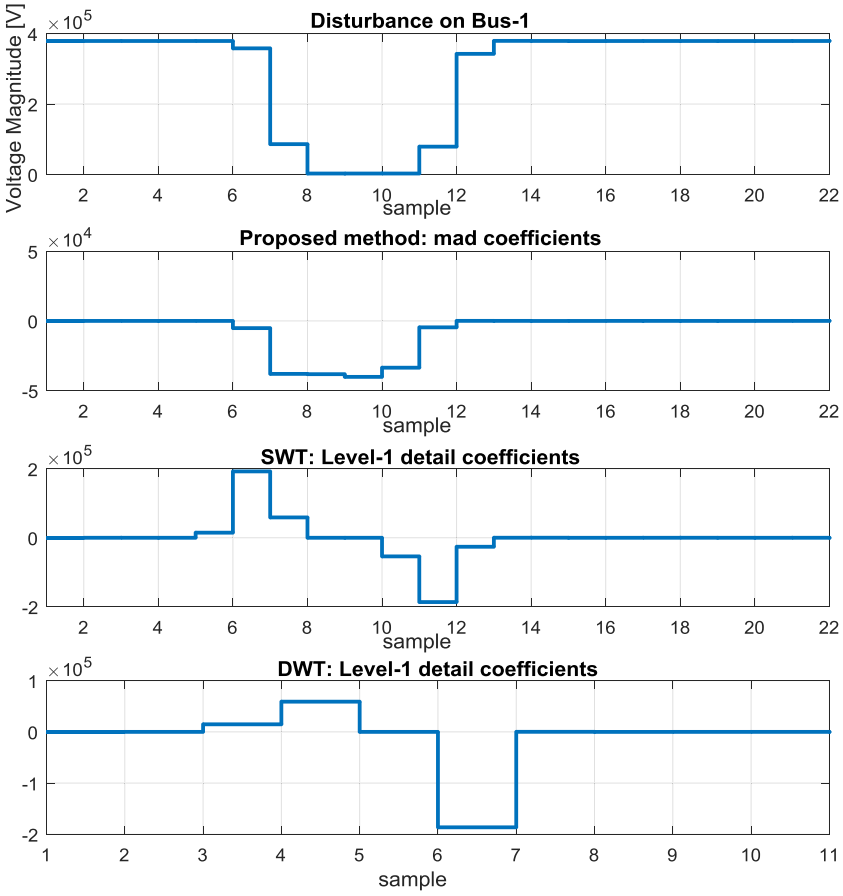

Fig. 8. Visual response comparison of the proposed, SWT, and DWT methods.

tion, which can be utilized as a standalone WAMPAC application or as a pre-step of AC and HVDC backup protection schemes. The applicability of the proposed method to detect disturbances in near real-time is verified by applying different faults, generation disconnection, and line trip on the AC and HVDC grid. Based on the performed simulations, the proposed algorithm has the following features and advantages:

a. low complexity of implementation,
b. fast response and low computational burden,
c. ability to detect all types of faults including a high-resistance fault with 1 ms duration,
d. robust to load fluctuations and noise,
e. applicable for disturbance detection in AC and HVDC.

Considering the modern small fiber optic telecommunication latencies, the proposed algorithm has practical merits in advanced protection schemes. Further research will be conducted to apply the proposed technique for the decentralized disturbance detection using recently introduced IEC 61869 based waveform measurements, where the issue of time delay will be investigated [35,36].

Funding

This work was financially supported by the Dutch Scientific Council NWO STW, under the project number “408-13-025” and in collaboration with TenneT TSO and the Dutch National Metrology Institute, van Swinden laboratory.

Acknowledgments

The authors very gratefully acknowledge the in-kind contributions of GE and SEL by the means of hardware and software respectively.

References

[1] R. Ma, H.-H. Chen, Y.-R. Huang, W. Meng, Smart grid communication: its challenges and opportunities, IEEE Trans. Smart Grid 4 (2013) 36–46.
[2] IEEE Standard for Synchrophasor Measurements for Power Systems — Amendment 1. Modification of Selected Performance Requirements, *IEEE Std C37.118.1a-2014 (Amendment to IEEE Std C37.118.1-2011)*, 2014; pp. 1–25.
[3] IEEE Standard for Synchrophasor Data Transfer for Power Systems, *IEEE Std C37.118. 2-2011 (Revision of IEEE Std C37.118-2005)*, 2011; pp. 1–53.
[4] A.G. Phadke, J.S. Thorp, Synchronized Phasor Measurements and Their Applications, vol. 1, Springer, 2017.
[5] V. Terzija, G. Valverde, D. Cai, P. Regulski, V. Madani, J. Fitch, S. Skok, M.M. Begovic, A. Phadke, Wide-area monitoring, protection, and control of future electric power networks, Proc. IEEE 99 (2011) 80–93.
[6] M. Liserre, T. Sauter, J.Y. Hung, Future energy systems: integrating renewable energy sources into the smart power grid through industrial electronics, IEEE Ind. Electron. Mag. 4 (2010) 18–37.
[7] D. Boroyevich, I. Cvetkovic, R. Burgos, D. Dong, Intergrid: a future electronic energy network? IEEE J. Emerg. Sel. Top. Power Electron. 1 (2013) 127–138.
[8] P. Pourbeik, P.S. Kundur, C.W. Taylor, The anatomy of a power grid blackout—root causes and dynamics of recent major blackouts, IEEE Power Energy Mag. 4 (2006) 22–29.
[9] IEEE Recommended Practice for Monitoring Electric Power Quality, *IEEE Std 1159–2009 (Revision of IEEE Std 1159–1995)*, 2009.
[10] M.V. Ribeiro, J. Szczupak, M.R. Iravani, I.Y.H. Gu, P.K. Dash, A.V. Mamishev, Emerging Signal Processing Techniques for Power Quality Applications, Springer, 2007.
[11] M.H. Bollen, I. Gu, Signal Processing of Power Quality Disturbances, vol. 30, John Wiley & Sons, 2006.
[12] H. Erişti, Ö. Yıldırım, B. Erişti, Y. Demir, Optimal feature selection for classification of the power quality events using wavelet transform and least squares support vector machines, Int. J. Electr. Power Energy Syst. 49 (2013) 95–103.

[13] Z.L. Gaing, Wavelet-based neural network for power disturbance recognition and classification, IEEE Trans. Power Deliv. 19 (2004) 1560–1568.
[14] M. Caujolle, M. Petit, G. Fleury, L. Berthet, Reliable power disturbance detection using wavelet decomposition or harmonic model based kalman filtering, 2010 14th International Conference on Harmonics and Quality of Power (ICHQP) (2010).
[15] K. Thirumala, A.C. Umarikar, T. Jain, Estimation of single-phase and three-phase power-quality indices using empirical wavelet transform, IEEE Trans. Power Deliv. 30 (2015) 445–454.
[16] M.S. Azam, F. Tu, K.R. Pattipati, R. Karanam, A dependency model-based approach for identifying and evaluating power quality problems, IEEE Trans. Power Deliv. 19 (2004) 1154–1166.
[17] S. Santoso, W.M. Grady, E.J. Powers, J. Lamoree, S.C. Bhatt, Characterization of distribution power quality events with Fourier and wavelet transforms, IEEE Trans. Power Deliv. 15 (2000) 247–254.
[18] S. Mishra, C.N. Bhende, B.K. Panigrahi, Detection and classification of power quality disturbances using S-transform and probabilistic neural network, IEEE Trans. Power Deliv. 23 (2008) 280–287.
[19] S. Suja, J. Jerome, Pattern recognition of power signal disturbances using S transform and TT transform, Int. J. Electr. Power Energy Syst. 32 (2010) 37–53.
[20] S. Mallat, W.L. Hwang, Singularity detection and processing with wavelets, IEEE Trans. Inf. Theory 38 (1992) 617–643.
[21] K. De Kerf, K. Srivastava, M. Reza, D. Bekaert, S. Cole, D. Van Hertem, R. Belmans, Wavelet-based protection strategy for DC faults in multi-terminal VSC HVDC systems, IET Gener. Transm. Distrib. 5 (2011) 496–503.
[22] L. Liu, M. Popov, M. Van Der Meijden, V. Terzija, A wavelet transform-based protection scheme of multi-terminal HVDC system, 2016 IEEE International Conference on Power System Technology (POWERCON) (2016).
[23] Y. Yang, T. Pierce, J. Carbonell, A study of retrospective and on-line event detection, Proceedings of the 21st Annual International ACM SIGIR Conference on Research and Development in Information Retrieval (1998).
[24] A.J. Allen, S.-W. Sohn, S. Santoso, W.M. Grady, Algorithm for screening PMU data for power system events, Innovative Smart Grid Technologies (ISGT Europe) (2012).
[25] S. Li, X. Wang, Monitoring disturbances in smart grids using distributed sequential change detection, 2013 IEEE 5th International Workshop on Computational Advances in Multi-Sensor Adaptive Processing (CAMSAP) (2013).
[26] J. Ma, Y.V. Makarov, R. Diao, P.V. Etingov, J.E. Dagle, E. De Tuglie, The characteristic ellipsoid methodology and its application in power systems, IEEE Trans. Power Syst. 27 (2012) 2206–2214.
[27] Y. Ge, A.J. Flueck, D.-K. Kim, J.-B. Ahn, J.-D. Lee, D.-Y. Kwon, Power system real-time event detection and associated data archival reduction based on synchrophasors, IEEE Trans. Smart Grid 6 (2015) 2088–2097.
[28] Y. Seyedi, H. Karimi, J.M. Guerrero, Centralized disturbance detection in smart microgrids with noisy and intermittent synchrophasor data, IEEE Trans. Smart Grid 8 (2017) 2775–2783.
[29] S. Maharjan, J.C.-H. Peng, J.E. Martinez, W. Xiao, P.-H. Huang, J.L. Kirtley, Improved sample value adjustment for synchrophasor estimation at off-nominal power system conditions, IEEE Trans. Power Deliv. 32 (2017) 33–44.
[30] C. Thilakarathne, L. Meegahapola, N. Fernando, Improved synchrophasor models for power system dynamic stability evaluation based on IEEE C37. 118.1 reference architecture, IEEE Trans. Instrum. Meas. 66 (2017) 2937–2947.
[31] C. Leys, C. Ley, O. Klein, P. Bernard, L. Licata, Detecting outliers: do not use standard deviation around the mean, use absolute deviation around the median, J. Exp. Soc. Psychol. 49 (2013) 764–766.
[32] M. Naglic, I. Tyuryukanov, M. Popov, M. Meijden, V. Terzija, WAMPAC-ready platform for online evaluation of corrective control algorithms, MedPower Conference (2016).
[33] CIGRE WG B4.57 Guide for the Development of Models for HVDC Converters in a HVDC Grid, *CIGRE WG B4.57, Technical Brochure*, vol. 604, 2014.
[34] M. Naglic, M. Popov, M.A.M.M. van der Meijden and V. Terzija, Synchro-Measurement Application Development Framework: An IEEE Standard C37.118.2-2011 Supported MATLAB Library, in IEEE Transactions on Instrumentation and Measurement doi: 10.1109/TIM.2018.2807000.
[35] S.M. Blair, A.J. Roscoe, J. Irvine, Real-time compression of IEC 61869-9 sampled value data, 2016 IEEE International Workshop on Applied Measurements for Power Systems (AMPS) (2016).
[36] IEC 61869-9: Digital interface for instrument transformers, Standard IEC 61869-9, 2016.

Matija Naglic received the Uni. Dipl.-Ing. degree in electrical engineering from the Faculty of Electrical Engineering, University of Ljubljana, Ljubljana, Slovenia, in 2012. He was a Researcher with the Milan Vidmar Electric Power Research Institute, Ljubljana, Slovenia. He is currently working toward the Ph.D. degree at the Intelligent Electrical Power Grids group, Delft University of Technology, Delft, The Netherlands. His research interests include real-time monitoring and control of large-scale power systems.

Lian Liu received his B.Sc. and M.Sc. degrees in electrical engineering from the Wuhan University, Wuhan, China, in 2010 and 2013, respectively. He is currently working toward the Ph.D. degree in the same field in Delft University of Technology, Delft, The Netherlands. His PhD project is financed by China Scholarship Council (CSC). His research interests include the modelling large scale of HVDC system, HVDC system transients and power system protection.

Ilya Tyuryukanov received the B.S.E.E. degree from Moscow Power Engineering Institute (Technical University), Moscow, Russia, and the M.Sc. degree from RWTH Aachen University, Aachen, Germany. He is currently working toward the Ph.D. degree at the Delft University of Technology, Delft, The Netherlands. His research interests include machine learning and optimisation techniques applied to power systems, in particular, wide-area control and protection.

Marjan Popov received the Dipl.-Ing. degree from the University of Skopje, Skopje, Macedonia, in 1993 and the Ph.D. degree in electrical power engineering from Delft University of Technology, Delft, The Netherlands, in 2002. In 1997, he was an Academic Visitor at the University of Liverpool, Liverpool, U.K., working in the arc research group on modeling SF6 circuit breakers. His major fields of interest are future power systems, large-scale power system transients, intelligent protection for future power systems, and wide-area monitoring and protection. Prof. Popov is also a member of CIGRE and actively participated in WG C4.502 and WG A2/C4.39. He is IEEE PES Prize Paper Award and IEEE Switchgear Committee Award recipient for 2011 and associate editor of the international journal of electric power and energy systems.

Mart A.M.M. van der Meijden received the M.Sc. degree (cum laude) in electrical engineering from the Eindhoven University of Technology, the Netherlands, in 1981. He is full professor (part-time) with the Department of Electrical Sustainable Energy of the Faculty of Electrical Engineering, Mathematics and Computers Science, Delft University of Technology, since June 2011. His chair and research focus is on Large Scale Sustainable Power Systems. Professor van der Meijden has more than 30 years of working experience in the field of process automation and the transmission and the distribution of gas, district heating and electricity. He is leading research programs on intelligent electrical power grids, reliable and large scale integration of renewable (wind, solar) energy sources in the European electrical power systems and advanced grid concepts. Since 2003 he is working with TenneT TSO, Europe's first cross-border grid operator for electricity. He is Manager R&D/Innovation and was responsible for the development of the TenneT long term vision on the electrical transmission system. Professor van der Meijden is member of IEEE, ENTSO-E/RDIC and CIGRE and he has joined and chaired different national and international expert groups.

Vladimir Terzija was born in Donji Baraci (former Yugoslavia). He received the Dipl-Ing., M.Sc., and Ph.D. degrees in electrical engineering from the University of Belgrade, Belgrade, Serbia, in 1988, 1993, and 1997, respectively. He is the Engineering and Physical Science Research Council Chair Professor in Power System Engineering with the School of Electrical and Electronic Engineering, The University of Manchester, Manchester, U.K., where he has been since 2006. From 1997 to 1999, he was an Assistant Professor at the University of Belgrade, Belgrade, Serbia. From 2000 to 2006, he was a senior specialist for switchgear and distribution automation with ABB AG Inc., Ratingen, Germany. His current research interests include smart grid application of intelligent methods to power system monitoring, control, and protection; wide-area monitoring, protection, and control; switchgear and fast transient processes; and digital signal processing applications in power systems.